

Dynamic Modes of Nanoparticle Motion During Nanoprobe-based Manipulation

Afshin Tafazzoli and Metin Sitti

Dept. of Mechanical Eng, Carnegie Mellon University, Pittsburgh, PA 15213, USA

Abstract — In this paper, dynamic behavior of nanoparticle motion during nanoprobe-based manipulation is investigated. Pushing, pulling or picking manipulation of the particles results in different behavior of rolling, sliding, sticking, or rotation. For a given point of contact of the nanoprobe tip on the particle, nanoprobe load magnitude and direction and critical frictional forces are obtained in all possible operation modes. Friction models in this paper considered both the normal and adhesion forces that are more general comparing to other papers. Pull-off forces in JKR model determine whether critical conditions are gained. Furthermore, developed mode diagrams, caused by the probe loading, indicate the possible dynamic behavior of nanoparticles. This would benefit us on tribological characterization of materials.

Index Terms — Atomic force microscopy, Nanorobotics, Nanomanipulation.

I. INTRODUCTION

Atomic force microscope (AFM) has evolved into a nanomanipulation tool besides of its 3D nanoscale imaging capabilities with atomic resolution. This study is focused on the analysis of nanoparticle dynamic motion modes during pushing the particle using an AFM nanoprobe. The behavior of the spherical nano-particles by controlling the probe tip force angle and magnitude is considered and compared for different dynamic motion modes.

II. METHOD

Two methods can be considered for pushing nanoparticles: (1) Moving substrate with a controlled constant speed while AFM probe is in contact with particle; (2) AFM probe tip moves and pushes the targeted particle over the immobile substrate. Even though they look different, dynamic results would be the same for both methods. We are using the second method where the probe forces (F_T) acting between the tip and the particle are kept constant (Figure 1).

Friction force is proportional to the real contact area and normal force, according to the Johnson-Kendall-Roberts (JKR) model [1]. Friction models for sliding, rolling, and spinning are then given as follow [2]:

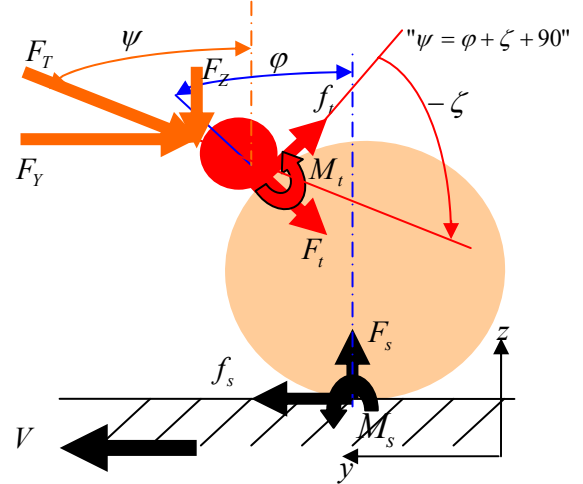


Figure.1 Forces during pushing a nanoparticle using an AFM probe tip modeled as a sphere

Sliding Friction:

$$f_s > \mu_s F_s + \tau_s A_s \quad (1)$$

$$f_t > \mu_t F_t + \tau_t A_t \quad (2)$$

Rolling Friction:

$$(f_s + f_t)R > M_{s_{\max}} + M_{t_{\max}} \quad (3)$$

$$M_{s_{\max}} = \mu_{r_s} F_s + \tau_{r_s} A_s \quad (4)$$

$$M_{t_{\max}} = \mu_{r_t} F_t + \tau_{r_t} A_t \quad (5)$$

Spinning Friction:

$$F_y x_0 > \mu_s F_s + \tau_s A_s \quad (6)$$

where μ is a friction coefficient, τ is a shear strength, A is a contact area, R is a nanoparticle radius, and x_0 is an offset along the x -axis [4].

Deriving force relations in quasi-static motion can be written in terms of probe force and angles:

$$f_t = F_T \cos \zeta \quad (7)$$

$$F_t = -F_T \sin \zeta \quad (8)$$

$$f_s = F_T \sin \psi \quad (9)$$

$$F_s = F_T \cos \psi \quad (10)$$

Considering Equations (1-10) and make all the substitutions, critical forces for sliding on tip, sliding on substrate, rolling, and spinning are derived as:

$$F_T > \frac{\tau_s A_s}{\sin \psi - \mu_s \cos \psi} (\equiv F_s^*) \quad (11)$$

$$F_T > \frac{\tau_t A_t}{\cos \zeta + \mu_t \sin \zeta} (\equiv F_t^*) \quad (12)$$

$$F_T > \frac{\tau_r A_s + \tau_r A_t}{R(\sin \psi + \cos \zeta) + \mu_r \sin \zeta - \mu_s \cos \psi} (\equiv F_r^*) \quad (13)$$

$$F_T > \frac{\tau_s A_s}{x_0 \sin \psi - \mu_s \cos \psi} (\equiv F_{cs}^*) \quad (14)$$

Therefore, F^* is a function of pushing force angle ψ , tip-particle contact angle ϕ , contact area A , and friction constants μ , τ . When F_T exceeds the critical force F^* determined by friction models, it is causing corresponding motion. Critical rolling force is inversely proportional to the radius of the particle R (Eq. 13). Applying a centered force ($x_0=0$) would reduce the possibility of undesirable separation of the particle due to spinning (Eq. 14).

Two important questions are: (1) what probe force is required to move the target nanoparticle?, and (2) which dynamic mode occurs first?

Dynamic behavior of nanoparticles is achieved by solving and plotting critical Equations (10-12). Sample mode diagrams are attached for different model configurations (Figures 2-5).

In a pushing zone ($\phi > 0$), particle sliding on the substrate occurs earlier than sliding on the tip which is opposite in a pulling zone ($\phi < 0$).

Required forces to separate two surfaces are mainly proportional to the equivalent radius R' and the surface energy γ between contacting surfaces [3].

$$F_{JKR}^* = -\frac{3}{2} \pi \gamma R \Rightarrow A^* = \pi a^{*2} = \pi \left(\frac{3\pi \gamma R^2}{2K} \right)^{\frac{2}{3}} \quad (15)$$

$$R' = \frac{RR_t}{R + R_t} \cong R_t \ll R \Rightarrow A_t \ll A_s \quad (16)$$

For this reason, critical force for slipping on the tip is less than other criteria (Eq. (16)). To insure the probe is in contact with particle during the pushing phase, the surface energy between probe tip and particle is increased (Figure 3).

Sliding occurs first and is more dominant to rolling in smaller particles (Figures 2-4). On the other hand, sliding and rolling could be observed simultaneously if the applied force increases above both critical limits. Required force for manipulating smaller particles is smaller, but to overcome the critical forces, a minimum manipulation force is required.

However, at load angles where critical forces are negative, friction condition is not satisfied and dynamic motion is not possible. Also at singular points (peaks), system become unstable that should be avoided.

To be more specific and better understand the dynamic behavior of the particles from mode diagrams, the above method is being limited to the working range with nanoparticles and nominal values are chosen as in Table 1:

Design Parameters (X)	Limit ($<X<$)		Nominal Value (X^*)
	Min	Max	
Radius (R [nm]); $R_t^*=20$ nm	10	5000	50
Surface Energy (γ [J/m^2])	0.1	2	0.2
Tip-Particle Force Angle (ψ [$^\circ$])	0	90	75
Tip-Particle Contact Angle (ϕ [$^\circ$])	0	90	60

Table 1 Model parameters

Mode diagrams (Figures 6-9) are plotted by having all the parameters fixed at their nominal values, and considering the variations in dynamic behavior due to small changes on design parameters.

At nominal values sliding on the substrate is dominant, and required force for sliding is about 7 nN (Figure 6).

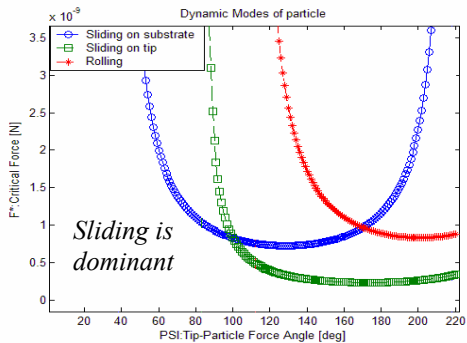
IV. CONCLUSIONS

According to the derived mode diagrams, dynamic behavior of nanoparticles can be predicted. Desired nanoparticle manipulation is provided by controlling the load and contact angle. This would enable us to tribologically characterize particle motion at the nano-scale.

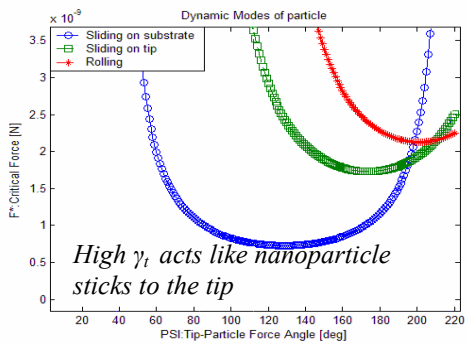
REFERENCES

- [1] B. Bhushan, Intro. to Tribology, John Wiley & Sons, New York, 2002.
- [2] K. L. Johnson, Contact Mechanics, Cambridge University, London, 1985.
- [3] S. Saito, H. T. Miyazaki, T. Sato, K. Takahashi, "Kinematics of mechanical and adhesional micromanipulation under a scanning electron microscope" *Journal of Applied Physics*, vol. **92**, no. 9, pp. 5140-49, November 2002.
- [4] M. Sitti, "Atomic force microscope probe based controlled pushing for nano-tribological characterization" *IEEE/ASME Transactions on Mechatronics*, vol. **9**, no. 2, June 2004 (to appear).

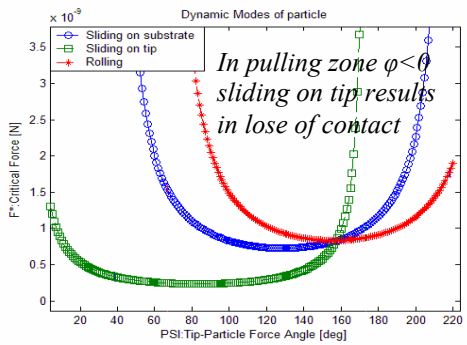
Figure 2-5: Critical force F^* values in terms of pushing force angle ψ to derive possible dynamic modes of nanoparticles; $R_t=15\text{ nm}$



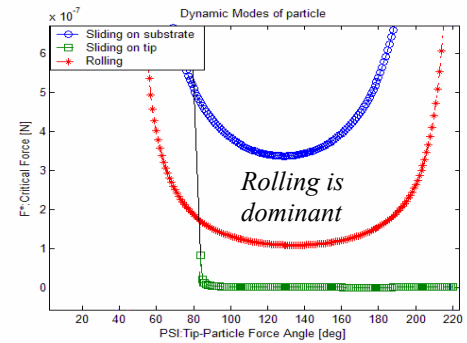
(2) $\phi = 45, R = 20\text{ nm}, \gamma_t = 0.1\text{ J/m}^2$



(3) $\phi = 45, R = 20\text{ nm}, \gamma_t = 2\text{ J/m}^2$

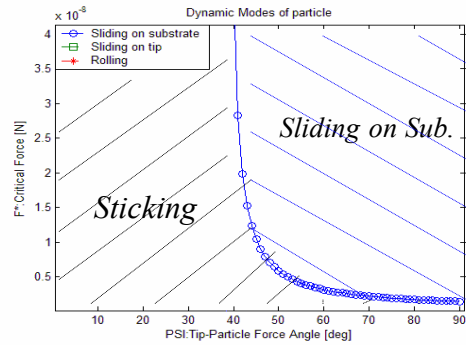


(4) $\phi = -45, R = 20\text{ nm}, \gamma_t = 0.1\text{ J/m}^2$

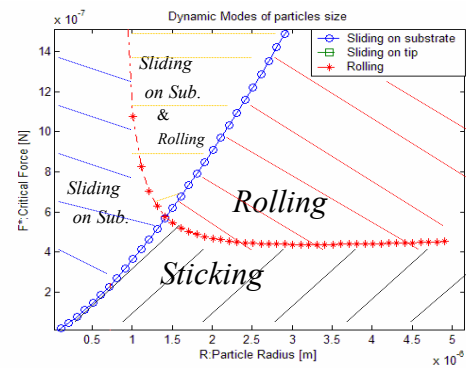


(5) $\phi = 45, R = 2000\text{ nm}, \gamma_t = 0.1\text{ J/m}^2$

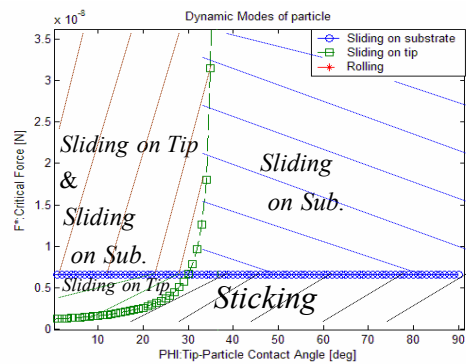
Figure 6-9: Mode diagrams (dashed lines show different dynamic regions) based on nominal values



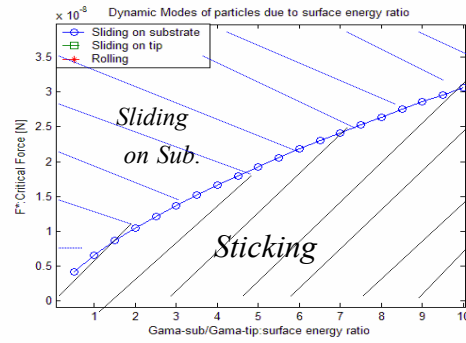
(6) $F^*(R^*, \gamma^*, \phi^*)$ for different ψ



(7) $F^*(\gamma^*, \psi^*, \phi^*)$ for different particle radii



(8) $F^*(R^*, \gamma^*, \psi^*)$ for different ϕ



(9) $F^*(R^*, \psi^*, \phi^*)$ for different surface energy